Turk J Phys
32 (2008) , 97 – 103.

Ac conductivity and Ultrasonic Studies in $KHCO_3$ Compound

Fathy SALMAN, Sayed ABOUELHASSAN, Eslam SHEHA and Mabrouk ELMANSY
Physics Department, Faculty of Science, Banha University-EGYPT
e-mail: fathy55555202@yahoo.com

Received 30.05.2007

Abstract

The total conductivity of $KHCO_3$ compound is studied in the frequency range 50 Hz–1 MHz and in the temperature range 300–370 K. The conductivity frequency dependence relation is divided into three regions: one at low frequency (dc conductivity), while the others appear at a moderate and relatively higher frequency range. In general, the conductivity frequency dependence conductivity obeys a double power law relation, $\sigma_{tot} = \sigma_{dc} + A\omega^p + B\omega^q$. The powers p and q have been found to be in the range 0 to 1 and 1 to 2, respectively. The attenuation coefficient β of $KHCO_3$ compound was studied over a temperature range from room temperature up to 370 K. The general behavior showed two essential activated regions. The activation energies are estimated and discussed.

Key Words: $KHCO_3$, Ac conductivity, Ultrasonic

1. Introduction

Potassium bicarbonate $KHCO_3$ belongs to the class of materials that are composed of hydrogen-bonded dimmers. These systems provide tools for investigating the properties of hydrogen bonding, which plays an important role in various aspects of the natural sciences, including the life science [1]. There has also been considerable interest in the order-disorder phase transitions of these materials. $KHCO_3$ undergoes antiferrodistortive phase transitions of order-disorder type at $T_c = 318$ K [2–5]. The general feature of the structure that was given earlier by Nitta et al [6] has been refined by three-dimensional X-ray diffraction [7] and also by neutron diffraction[8]. Accordingly, the crystals are monoclinic, space group $P2_1/a$ with cell dimensions $a = 1.51725$, $b = 0.56283$, $c = 0.37110$ nm, and $\beta = 104.631^o$. Spectroscopy studies [9-11], NMR [12, 13] and quasi-elastic neutron scattering [14] converge to the conclusion that proton transfer occurs via tunneling across a quasi-symmetric double minimum potential. Two stochastic mechanisms have been proposed: pair-wise synchronous transfer, and the uncorrelated two-stepwise single proton transfer. The $(KHCO_3)_2^-$ dimer in $KHCO_3$ is partially disordered at room temperature because of the two equilibrium positions of hydrogen. According to Kashida and Yamamoto [2], the hydrogen atoms occupy the two equilibrium positions with half occupancies in the high-temperature phase, whereas in the low-temperature phase they are almost localized at one site. They conclud that the phase transition can be described in terms of order-disorder of the $(KHCO_3)_2^-$ dimers.

Association of the dynamic transfer of hydrogen atoms with structural phase transition has been the subject of keen interest. Yet, special attention should be paid to determine the ac conducting properties

of glasses which provide additional structural information [15, 16]. From ac conductivity studies, the low frequency measurements give useful insight into the mobile ion diffusion and high frequency conductivity data help us to investigate the short time phenomena due to the local motion of mobile ions. The present study has been undertaken to investigate the conductivity as a function of frequency and temperature of $KHCO_3$. The attenuation coefficient β of $KHCO_3$was studied over a temperature range from room temperature to 370 K to throw more light on transition of such material.

2. Experimental Technique

A finely grounded powder of the material ($KHCO_3$) was compressed under a suitable pressure (300 kg/cm^2) to form discs of diameter 1 cm and of thickness 1.5 mm. Good contact was attained by painting both faces of the sample with air drying conducting silver paste. The sample was held between two spring loaded electrodes was specially designed to fit the present electrical measurements. The conductivity was measured by means of a Hioki 3532-50 Hi-tester RCL meter controlled via a personal computer in the frequency range 50 Hz to 1 MHz and temperatures range 300 to 370 K.

For attenuation coefficient β measurement, samples in the form of rectangular of thickness 3 mm were used. The sample was fixed between two identically ultrasonic transducers in the attenuation holder and heated in an electrical furnace in a temperature range 300–370 K. The rate of heating was adjusted to be 2 K/min. The method used for the attenuation coefficient measurement is called a through transmission technique[17].

3. Results and Discussion

3.1. Frequency Dependence of the Electrical Conductivity

Figure 1 shows frequency dependence of the electrical conductivity of $KHCO_3$ compound at different ambient temperatures. It is noticed that the graphs show two threshold frequencies, ω_1 and ω_2, which separates the graphs into three regions, hence three conduction mechanisms. These graphs can be fit to the equation

$$\sigma_{tot} = \sigma_{dc} + A\omega^p + B\omega^q \tag{1}$$

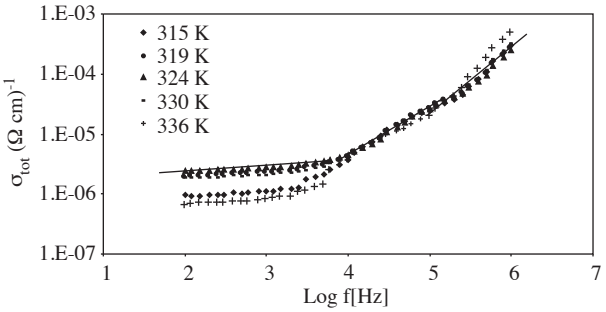

Figure 1. Frequency dependence of the total conductivity in $KHCO_3$ compound at various temperatures.

In the first region ($\omega < \omega_1$), σ_{dc} lies in the low frequency range, where we have found that σ_{tot} is independent of ω, representing σ_{dc} (extrapolation of σ_{tot} at $\omega = 0$). The values of σ_{dc} are plotted against the inverse of temperature, as shown in Figure 2. The variation of ln σ_{dc} against $1/T$ yield two straight lines of two different slopes at the temperature ranges 298–322 and 322–370K (see Figure 2). The values of E_1 and E_2 are found to be 1.9 eV and 1.7 eV for the lower and higher temperatures, respectively.

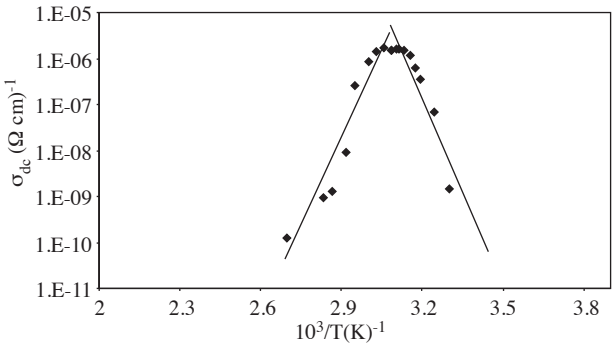

Figure 2. Variation of dc conductivity (extrapolation of σ_{tot} at $\omega = 0$) with temperature.

The theoretical approaches of this behavior may be explained via the understanding that the transport takes place through infinite percolation path [18]. The second region lies in the frequency range $\omega_1 < \omega < \omega_2$, where the general behavior of σ_{ac} is increasing with frequency obeying a power law: $\sigma_{ac} = A\omega^p$ where A is a temperature dependence term and p is the frequency exponent. The exponent p corresponds to the transnational hopping and/or reorientation motion and varies with temperature from 0 to 1. The estimated values of p as a function of temperature are given in Figure 3a. The temperature dependence of p shows a decreasing behavior but at certain temperature (T_F) it tends to increase. The third region lies in frequency range $\omega_2 \quad < \omega$, where the general behavior of σ_{ac} is increasing with frequency obeying a power law: $\sigma_{ac} = B\omega^q$, where B is a temperature dependent term and q is the frequency exponent. The exponent q corresponds to localized hopping motion and varies with temperature from 1 to 2. The estimated values of q as a function of temperature are given in Figure 3b. The temperature dependence of q shows decreasing behavior but at certain temperature T_F it tends to increase and decrease again at high temperatures. This behavior indicates the presence of two types of processes, which control the mechanism of the ac-conductivity behavior.

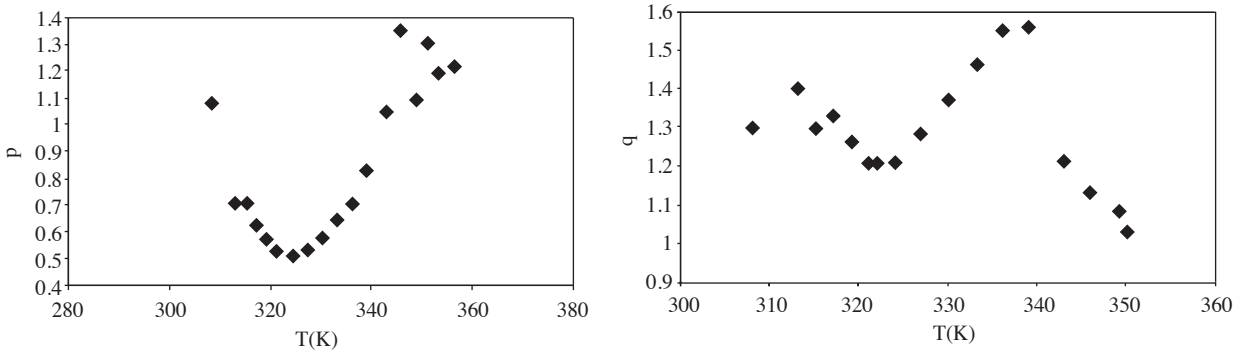

Figure 3. Temperature dependence of powers for $KHCO_3$ crystal (a) power p (b) power q.

The first type is responsible for the decreasing of a power; which suggests the barrier hopping of the ions through defects be involved in the conduction mechanism. The dispersion behavior is attributed to the coulomb interaction effects between the mobile ions as well as the ions with the environment within materials [19]. On the other hand the second type of mechanism is responsible for the increasing of a power; which agrees with the mechanism proposed by the quantum mechanical tunneling model (QMT)[20] where the temperature dependence of frequency exponent could arise from (QMT) model where the carrier motion occurs within clusters.

3.2. Temperature Dependence of ac Conductivity

The variations of the total conductivity with the inverse of temperature at different frequencies are given in Figure 4. From the figure it can be noticed that the ac conduction, at low frequency range (below 6 kHz),

consists of two types of conduction. In the first one, associated with the first arm at low temperature range, the ac conductivity increases linearly as the temperature was increased while, in the second arm at relatively high temperature, the ac conductivity starts to decrease linearly as the temperature increased. This may be attributed to that the ac conduction at low frequency controlled by the same processes of dc conductivity.

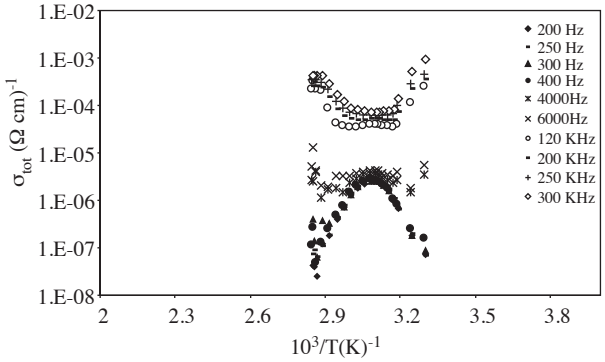

Figure 4. Temperature dependence of the total conductivity in $KHCO_3$ compound at different frequencies.

Figure 4 shows two types of ac conduction in the high frequency range. In the first one, associated with the first arm in the low temperature range, the ac conductivity decreases linearly with temperature increase, which may be in the high frequency, a considerable number of dipoles can't flip to the opposite direction and the deviations of dipole moments become small. This means that the life time of a dipole becomes long and the transfer of a proton between two sites does not occur frequently [21]. Therefore, the movements of the protons into neighboring dimers will not contribute to the conduction mechanism and charge carrier-phonon scattering dominates. In the second type of conduction, associated with the second arm at high temperature range, the ac conductivity increases linearly which may be attributed to thermally activated process of dipoles to flip at high temperature range. Therefore, a considerable number of dipoles able to flip to the opposite direction and the deviations of dipole moments become large. This means that the life time of a dipole becomes short and the transfer of a proton between two sites occurs frequently. Therefore, the movements of the protons into neighboring dimers will contribute to the conduction mechanism reflecting the increase of ac conductivity as the temperature was increased. The activation energy of conduction and charge carrier scattering corresponding to different temperatures and frequencies has been calculated and listed in Table. From this Table it can be noticed that activation energy decreases with increasing frequency.

The change of the values of the activation energies is taken as evidence of the existence of a phase transition [22]. The decreasing in the activation energy may be interpreted in terms of the transition in the sample from order-disorder and from disorder-order phase.

The $(HCO_3)_2$ dimer consists of two HCO_3^- ions linked by two hydrogen bonds [14]. The population of protons in the ground state decreases with increasing temperature, due to the excitation of protons to the excited states. Also, the proton movement into neighboring dimers and correlated reorientation of the latter will contribute to the conduction mechanism [21]. While the decrease of σ_{dc} with increasing temperature (second range) may be attributed to the expected increase in the number of the scatters (phonon modes) in the high temperature range, the scattering mechanism of the charge carries increase which lead to decrease in the conduction mechanism.

From the above discussion one can conclude that the charge carrier hopping rate between two adjacent filled and empty sites depends on: (i) phonon charge carrier coupling; (ii) the hopping distance between filled and empty sites; and (iii) applied electric field direction and frequency.

Table. Activation energies for $KHCO_3$ before and after the transition temperature and at low and high frequencies.

Frequency, Hz	Activation energies of conduction before transition, eV	Activation energies of attenuation before transition, eV
300	1.59	1.09
600	1.18	0.66
1000	0.86	0.75
1500	0.7	0.64
2500	0.14	0.05
5000	0.08	0.03
Frequency, Hz	Activation energies of attenuation before transition, eV	Activation energies of conduction before transition, eV
100	1.11	0.76
200	0.94	0.75
500	0.93	0.75
600	0.91	0.66
800	0.84	0.63
1000	0.29	0.55

3.3. Ultrasonic attenuation Coefficient Results

The anomalous elastic behavior using ultrasonic methods between 250 and 350 K was investigated by Hassuhl [23]. The phase transition in our $KHCO_3$ crystal sample was followed up with an examination of the attenuation coefficient β under ultrasound. Figure 5 shows the temperature dependence of β in the temperature range 298–385 K. From the graph it is clear the β-T relation is distinct in three regions. The region 298–313 K is temperature independent. In the second region, 313–343 K, the attenuation coefficient shows a sharp increase through a narrow temperature range, indicating the presence of some thermally activated process. The third region is characterized by temperature independence behavior.

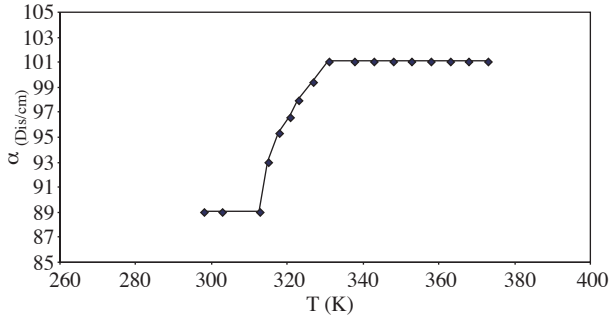

Figure 5. Temperature dependence of attenuation coefficient b through the transition region.

Many investigators [21, 22, 23] concluded that the hydrogen occupy two equilibrium positions in $KHCO_3$, with half occupancies in the high temperature range, while they are almost localized in one site in the low-temperature range. Hence, the phase transition can be described within the framework of the order-disorder of dimers, i.e. from monoclinic space group $P2_1/a$ to monoclinic space group C_2/m. Therefore the sharp increase in β can be attributed to the large scale availability of ultrasonic wave scattering on the dimers. Moreover, the large value of attenuation coefficient above T_F may be attributed to the increase of lattice vibration waves amplitude where the spontaneous strain above T_F is removed [24]. It has been found that thermal activation of β in the transition region can be explained by the following Arrehenus equation:

$$\beta = \beta_o e^{\Delta Ea/kT}, \tag{2}$$

where β_o is a pre-exponent constant, k is Boltzmann's constant and E_a is the attenuation activation energy. The relation between ln β and $1/T$ yield two straight-lines (see Figure 6) these lines are separated by a kink at the transition temperature $T_F = 322$ K, in agreement of the dc conductivity and dielectric properties [16]. The deduced activation energy of attenuation for the two regions in the former ranges of temperature are found to be 0.11 and 0.04 eV respectively. The obtained two different activation energies (0.11 and 0.04 eV) can be attributed to two mechanisms associated with ferroelastic phase transition, the dimer release randomly and crystal lattice parameters enlargement, respectively.

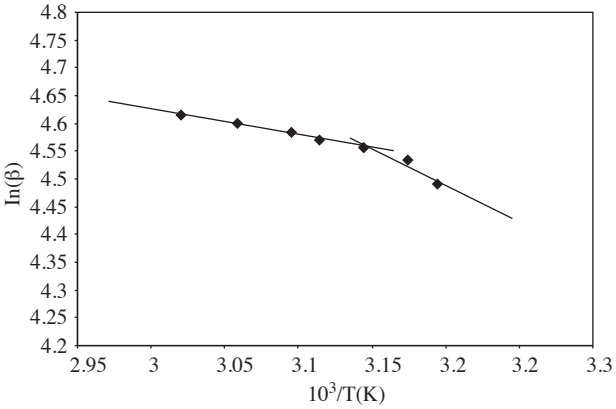

Figure 6. The variation of the attenuation coefficient (b) with the inverse of temperature for $KHCO_3$.

From the above discussion it can be concluded that the ultrasonic propagation in samples confirms the phase transition in $KHCO_3$ compound.

References

[1] R. Kanao, S. I. Nohdo, N. Horiuchi, S. Kashida, K. Kakurai, Y. Yamada, *J. Phys. Soc. Japan,* **65**, (1996), 1710.

[2] S. Kashida, K. Yamamoto, *J. Solid State Chem.*, **86**, (1990), 180.

[3] M. Machida, Y. Yamaguchi, M. Sugiyama, Y. Iwata, N. Koyano, S. Fukui, *Physica,* **B213**&**214**, (1995), 393.

[4] R. Kanao, S. I. Nohdo, N. Horiuchi, S. Kashida, K. Kakutai, Y. Yamada, *J. Phys. Soc. Japan*, **64**, (1995), 2286.

[5] K. Kakurai, T. Sakaguchi, M. Nishi, C.M.E. Zeyen, S. Kashida, Y. Yamada, *Phys. Rev.,* **B 53**, (1996), R5974.

[6] I. Nitta, Y. Tommie, and C. Hoe Koo, *Acta. Cryst.,* **5**, (1952), 292.

[7] J. Tomas, R. Tellgren and I. Olovsson, *Acta Cryst.,* **B30**, (1974), 1155.

[8] J. Thomas, R. Tellgren and I. Olovosson, *Acta Cryst.,* **B30**, (1974), 25 40.

[9] F. Fillaux, *Chem. Phys.,* **74**, (1983), 405.

[10] S. Ikeda, F. Fillaux, *Phys. Rev.,* **B59**, (1999), 4134.

[11] F. Fillaux, A. Cousson, D. Keen, *Phys. Rev.*, **B67**, (2003), 54301.

[12] S. Benz, U. Haeberien, J. Tegenfeldt, *J. Magn. Reson.*, **66**, (1986), 125.

[13] C. Odin, *J. Phys. Chem.*, **B108,** (2004), 7402.

[14] G. Eckold, H. Grimm and M. Stean-Arsic, *Physica,* **B180&181**, (1992), 336.

[15] J. Kawamura, M. Shimoji, *J. Non-Crys. Solids,* **79**, (1986), 367.

[16] F. Salman, S. Aboelhassan, E. Sheha, M. K. ElMansy, *Turk. J. Phys.,* **28**, (2004), 57.

[17] R. Truell, B. Celbaum, B. Chick, Ultrasonic Methods in Solids State Physics, Academic Press, (New York and London, 1969), p. 57.

[18] J. C. Dyre, *J. Appl. Phys.*, **64**, (1988), 2456.

[19] R. H. Chen, C. S. Shern, T. Fukami, *Journal of physics and Chemistry of Solids,* **63**, (2002), 203.

[20] Chanku lee, Sudac Lee, Chungsik Sul and Schwan Bae, *Physica*, **B239,** (1997), 316.

[21] Ahmed Ibrahim, Bum Suk KIM and Insuk Yu*, Journal of the Korean Physical Society,* **35**, (1999), 1419.

[22] M. M. Abdel-Kader, M. Fadly, M. Abutaleb, K. Eldehamy and A. I. Ali, *Phys. Stat. Sol. (a)*, **142**, (1994), 69.

[23] S. Haaussuhl, *Solid State Commun.*, **17**, (1986), 643.

[24] G. Eckold, H. Grimm and M. Stean-Arsic, *Physica*, **B180&181**, (1992), 336.